ACS Partner Journal

CHEM & BIO ENGINEERING

Open Access

This article is licensed under CC-BY-NC-ND 4.0

pubs.acs.org/ChemBioEng

Article

A Pillared-Layer Coordination Network for One-Step Ethylene Production from Ternary $CO_2/C_2H_2/C_2H_4$ Gas Mixture

Published as part of Chem & Bio Engineering special issue "Advanced Separation Materials and Processes".

Rong Yang,[+] Tao Zhang,[+] Jinbo Wang, Xue Zhang, Jian-Wei Cao, Yu Wang, and Kai-Jie Chen*

Cite This: *Chem Bio Eng.* 2025, 2, 35−40

Read Online

ACCESS | Metrics & More | Article Recommendations | Supporting Information

ABSTRACT: One-step separation of ethylene (C_2H_4) from multicomponent mixtures poses significant challenges in the petrochemical industry due to the high similarity of involved gas molecules. Herein, we report a pillared-layer coordination network named **Zn-fa-mtrz** (H_2fa = fumaric acid; Hmtrz = 3-methyl-1,2,4-triazole) possessing pore surfaces decorated with methyl groups and electronegative N/O atoms. Molecular modeling reveals that the pore surface of **Zn-fa-mtrz** provides more and stronger multiple interaction sites to simultaneously enhance the adsorption affinity for CO_2 and C_2H_2 other than C_2H_4. The experimental and simulated breakthrough experiments demonstrate the ability to produce high-purity C_2H_4 (>99.97%) in one-step from ternary $CO_2/C_2H_2/C_2H_4$ gas mixtures.

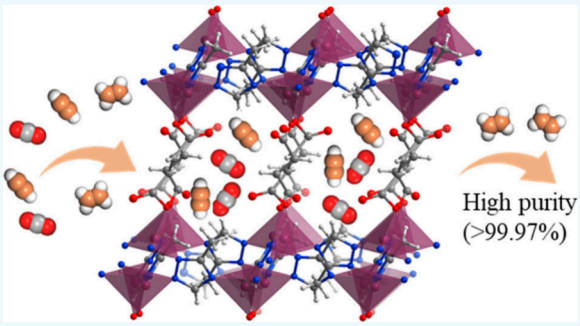

KEYWORDS: *adsorption separation, ethylene production, pore engineering, metal−organic frameworks, coordination network*

1. INTRODUCTION

Ethylene (C_2H_4) is one of the most important basic chemicals in the petrochemical industry, with an annual output of 214 million tons in 2021.[1,2] In the petrochemical process (i.e., steam cracking of naphtha) of C_2H_4 production, carbon dioxide(CO_2) and acetylene (C_2H_2) are the main impurities in the downstream gas mixture.[3,4] Thus, efficient removal of these impurities from related gas mixtures is very important in the chemical industry. The conventional technology used to remove C_2H_2 and CO_2 for C_2H_4 purification relies on catalytic hydrogenation for C_2H_2 removal and caustic soda absorption for CO_2 removal, which are sophisticated and highly energy-intensive.[5] Hence, it is urgent to develop a simple, effective, and energy-efficient C_2H_4 purification technology for such a requirement.

Physisorbent-based separation technology is a promising alternative to effectively separate and purify hydrocarbon mixtures, thanks to the fast kinetics and low regeneration cost.[6−11] Removing C_2H_4 from complex systems in one step will simplify the separation process and further reduce the total energy. In this context, metal−organic framework (MOF),[12,13] also known as porous coordination polymer (PCP)[14,15]/metal−organic materials (MOMs)[16] have made considerable achievements on efficient separation of C_2H_4 from binary C2 hydrocarbons, such as C_2H_4/C_2H_6,[17−23] C_2H_2/C_2H_4.[24−33] However, the one-step separation of C_2H_4 from ternary $CO_2/C_2H_2/C_2H_4$ mixtures is still in its infancy stage. The main obstacle here is the highly similar molecular sizes (kinetic diameter: C_2H_2, 3.3 Å; CO_2, 3.3 Å; C_2H_4, 4.16 Å) and physicochemical properties (boiling point: C_2H_2, 188.4 K; CO_2, 194.7 K; C_2H_4, 169.4 K; quadruple moment: C_2H_2, 33.3 × 10^{-25} e.s.u. cm^2; CO_2, 29.1 × 10^{-25} e.s.u. cm^2; C_2H_4, 42.5 × 10^{-25} e.s.u. cm^2)[34−36] in this separation system, which will require the specific recognition sites to simutaneously capture CO_2 and C_2H_2. To date, very limited materials have been reported for the effecient separation of C_2H_4 from ternary $CO_2/C_2H_2/C_2H_4$ mixtures in one single step.[28,37−42] Furthermore, the deep understanding of multigas interaction mechanism and discovering the advanced porous materials with better performance is still highly desired.

Herein, a pillared-layer coordination network, $[Zn_2(fa)(mtrz)_2]$ (named as **Zn-fa-mtrz**), featuring accessible O/N adsorption sites and methyl groups, was constructed for this purpose. The specific pore structure affords the selective adsorption of CO_2 and C_2H_2 over C_2H_4. The favorable binding interaction sites in **Zn-fa-mtrz** for simultaneously strong adsorption of CO_2 and C_2H_2 over C_2H_4 is the key factor, based on the molecular simulation results. Also, the ability of such a material to produce ethylene from equimolar binary

Received: June 9, 2024
Revised: August 19, 2024
Accepted: August 21, 2024
Published: August 27, 2024

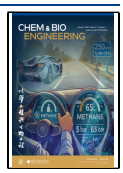

ACS Publications

© 2024 The Authors. Co-published by Zhejiang University and American Chemical Society

https://doi.org/10.1021/cbe.4c00113
Chem Bio Eng. 2025, 2, 35−40

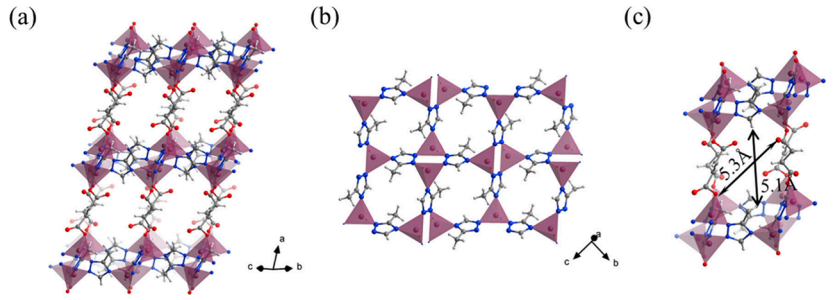

Figure 1. (a) Perspective view of the structure along the 1D channels of **Zn-fa-mtrz**. (b) The structure of the zinc-triazolate layer. (c) The maximum pore window of **Zn-fa-mtrz**. Color code: Zn, purple; C, gray; O, red; N, blue; H, white.

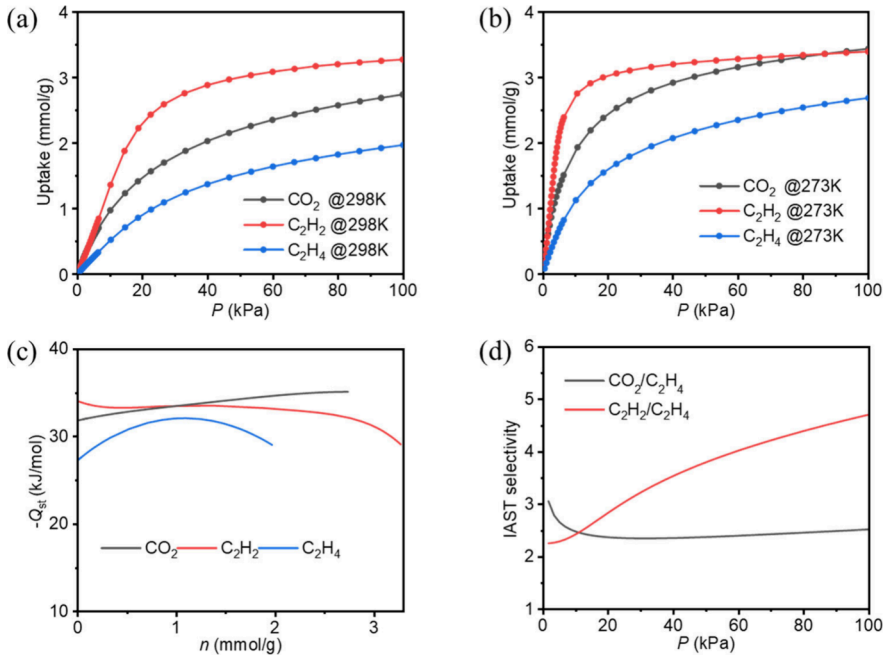

Figure 2. CO_2, C_2H_2, and C_2H_4 adsorption isotherms at 298 K (a) and 273 K (b); (c) the isosteric enthalpies of CO_2, C_2H_2, and C_2H_4 based on adsorption isotherms at three different temperature (273, 298, and 313 K), respectively; (d) IAST selectivity for equimolar binary gas mixture of CO_2/C_2H_4 and C_2H_2/C_2H_4 in **Zn-fa-mtrz**.

CO_2/C_2H_4 and C_2H_2/C_2H_4 mixtures, ternary $CO_2/C_2H_2/C_2H_4$ mixtures (1/1/1 and 9/1/90, *v*/*v*/*v*) in one step at room temperature is validated by experimental and simulated breakthrough techniques.

2. RESULTS AND DISCUSSION

Square-shaped crystals of **Zn-fa-mtrz** can be harvested through solvothermal reactions (Figure 1a) (see Supporting Information for detailed synthesis procedures). Single crystal X-ray diffraction data reveals that **Zn-fa-mtrz** crystallizes in the monoclinic $P2_1/c$ space group (Table S1), which is isostructural to the networks reported by our research group.[43,44] The asymmetric unit of **Zn-fa-mtrz** includes one four-coordinated Zn^{2+} ion, one-half fa^{2-} ligand, and one $mtrz^-$ ligand. The fa^{2-} and $mtrz^-$ ligands contain two uncoordinated carboxyl O atoms and one methyl group on the triazole ring. In **Zn-fa-mtrz**, triazole rings connects the dinuclear zinc units to form a wavy two-dimensional (2D) layer (Figure 1b). Such layers are bridged by fa^{2-} pillar ligands to afford a 3D **pcu** network. The porosity of **Zn-fa-mtrz** was calculated to be 38.1% (by PLATON[45]). The network contains a one-dimensional pore channel with a maximum pore window size of 5.3 Å × 5.1 Å (excluding the van der Waals radii) (Figure 1c), slightly larger than the kinetic dimensions of these target gas impurities, which is suitable for C_2H_4 purification. The network displays the specific cavity built by the presence of methyl groups and abundant uncoordinated negatively charged O/N atoms from layer and pillar ligands, which are all suitable potential hydrogen bond acceptors. These features are promising for the selective recognition of C_2H_2 and CO_2.

Powder X-ray diffraction (PXRD) patterns of the as-synthesized sample matched well with simulated patterns from the crystal structure, indicating the phase purity of the **Zn-fa-mtrz** sample (Figure S1). Thermogravimetric analysis (TGA) of **Zn-fa-mtrz** verified its thermal stability up to ca. 350 °C. The obvious weight loss in the TGA curve of as-synthesized sample before 210 °C is due to the release of solvent molecules (Figure S2). **Zn-fa-mtrz** can be fully exchanged with MeOH, as demonstrated by the PXRD patterns and TGA curves (Figures S1 and S2).

The permanent porosity of **Zn-fa-mtrz** was established by a reversible type-I N_2 sorption experiment at 77 K (Figure S3). The Brunauer−Emmett−Teller (BET) surface area for **Zn-fa-mtrz** is 633.3 $m^2\ g^{-1}$ (Figure S4). The saturated adsorption

https://doi.org/10.1021/cbe.4c00113
Chem Bio Eng. 2025, 2, 35−40

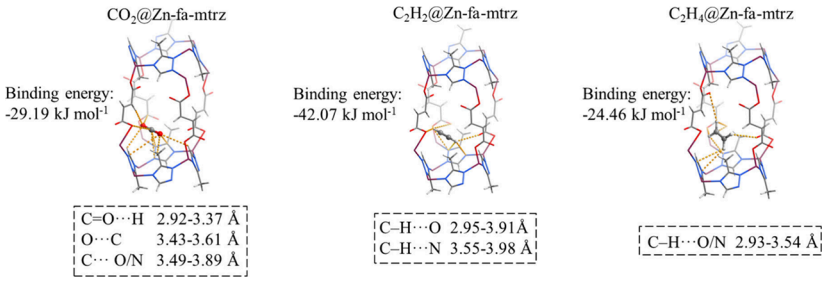

Figure 3. Preferential binding sites of CO_2, C_2H_2 and C_2H_4 in **Zn-fa-mtrz**. The guest-network interactions are highlighted in orange dashed bonds. Color code: Zn, purple; C, gray; O, red; N, blue; H, white.

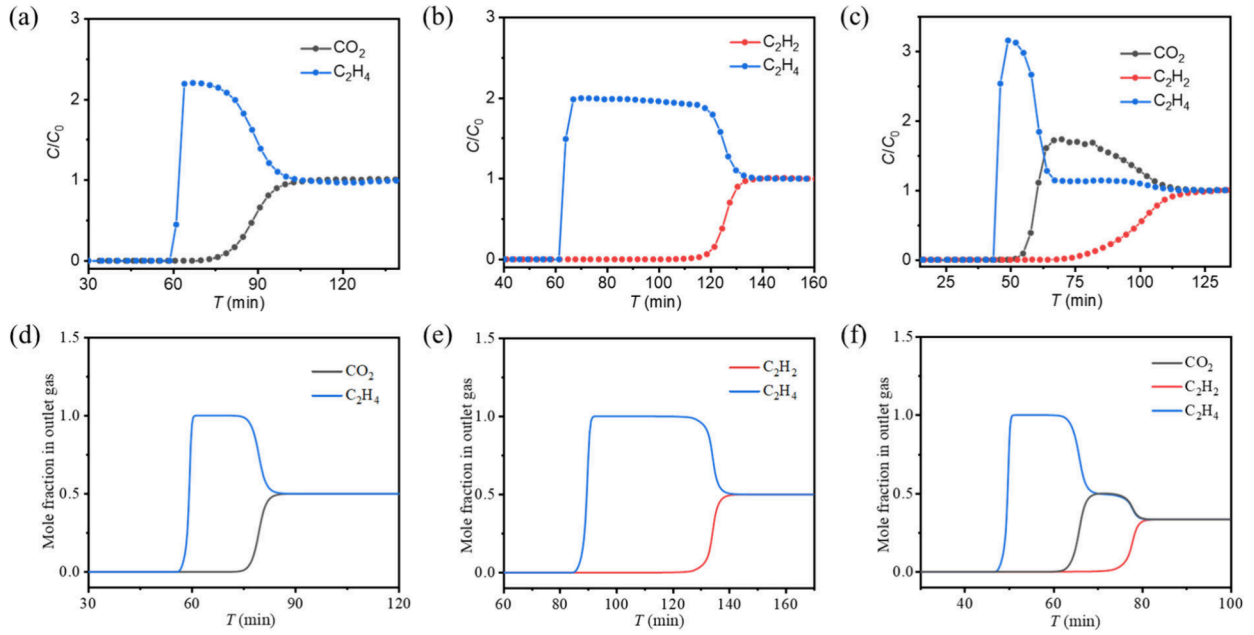

Figure 4. Experimental breakthrough curves of **Zn-fa-mtrz** at 298 K for (a) CO_2/C_2H_4 (1/1, *v*/*v*) (flow rate: 1.4 mL/min), (b) C_2H_2/C_2H_4 (1/1, *v*/*v*) (flow rate: 1.4 mL/min; total pressure: 1 bar), and (c) $CO_2/C_2H_2/C_2H_4$ (1/1/1, *v*/*v*/*v*) (flow rate: 2.1 mL/min). The simulated breakthrough curves at 298 K for (d) CO_2/C_2H_4 (1/1, *v*/*v*), (e) C_2H_2/C_2H_4 (1/1, *v*/*v*), and (f) $CO_2/C_2H_2/C_2H_4$ (1/1/1, *v*/*v*/*v*).

amount of the 77 K N_2 adsorption isotherm is 7.1 mmol g^{-1} at P/P_0 = 0.95. The experimental pore volume was estimated to be 0.245 cm^3 g^{-1}, which is comparable with the theoretical value of 0.287 cm^3 g^{-1} obtained from the crystal structure (Table S2). In addition, it is worth mentioning that **Zn-fa-mtrz** retains its crystalline and porosity after water treatment or exposure to humidity (ca. 53% RH) (Figure S5). The corresponding average pore size distribution based on the Horvath−Kawazoe model is approximately 5.7 Å, which is consistent with the pore size measured from the single-crystal structure.

The adsorption isotherms of CO_2, C_2H_2, and C_2H_4 for **Zn-fa-mtrz** were collected at 298 and 273 K (Figures 2a and 2b). At the low-pressure region, **Zn-fa-mtrz** demonstrates higher adsorption capacities for CO_2 and C_2H_2 than C_2H_4 (Figure 2a). Furthermore, the slopes of adsorption curves for CO_2 and C_2H_2 are greater than that of C_2H_4, indicating the stronger binding between CO_2 and C_2H_2 and the network. These results suggested selective adsorption of **Zn-fa-mtrz** toward CO_2 and C_2H_2 over C_2H_4. Notably, the uptake values of C_2H_2 (3.27 mmol g^{-1}) and CO_2 (2.74 mmol g^{-1}) at 298 K and 100 kPa significantly surpass that of C_2H_4 (1.97 mmol g^{-1}). To intuitively assess the interactions between the framework and gas molecules, the adsorption enthalpy (Q_{st}) for CO_2, C_2H_2, and C_2H_4 in **Zn-fa-mtrz** were calculated based on single-component adsorption data collected under 273, 298, and 313 K by utilizing the virial eq (Figures S6 and S7). The sequence of the adsorption affinity values follows the trend of C_2H_2 (−34.1 kJ mol^{-1}) > CO_2 (−31.8 kJ mol^{-1}) > C_2H_4 (−27.2 kJ mol^{-1}) at low loading (Figure 2c and Table S3), which is consistent with the adsorption uptake sequence and the slope of the isotherms. This phenomenon has also appeared in previous literature.[46,47] This demonstrates the apparently stronger binding affinity of **Zn-fa-mtrz** toward CO_2, and C_2H_2 as compared to C_2H_4.

To assess the separation ability, the selectivity of **Zn-fa-mtrz** for binary CO_2/C_2H_4, and C_2H_2/C_2H_4 mixtures were then calculated using ideal adsorption solution theory (IAST) based on the single-component adsorption isotherms at 298 K fitted by the dual-site Langmuir−Freundlich (DSLF) model (Figure S8 and Table S4). Under 100 kPa, the IAST values for equimolar CO_2/C_2H_4 and C_2H_2/C_2H_4 mixtures are 2.5 and 4.7, respectively (Figure 2d and (Table S5), which are comparable to the benchmark porous materials with C_2H_4 separation ability from three-component gas mixtures, such as **Zn-atz-oba** (CO_2/C_2H_4, 1.33, C_2H_2/C_2H_4, 1.43)[43] and **Zn-fa-atz (2)** (CO_2/C_2H_4, 1.4, C_2H_2/C_2H_4, 1.6).[44] The high selectivity displayed indicates the great potential of **Zn-fa-**

https://doi.org/10.1021/cbe.4c00113
Chem Bio Eng. 2025, 2, 35−40

mtrz for one-step C_2H_4 purification from ternary $CO_2/C_2H_2/C_2H_4$ mixtures under ambient conditions.

To fully understand the adsorption mechanism of these three gas molecules, Grand Canonical Monte Carlo (GCMC) simulations were performed to reveal the first favorable binding sites between **Zn-fa-mtrz** and gas molecules (see SI for simulation detail, Figure S9). As shown in Figure 3, all of these gas molecules are likely interacting with the framework at the corner formed by the fa^{2-} linkers and $mtrz^-$ ligands. C_2H_2 interacts with fa^{2-} linkers and $mtrz^-$ ligands via four C−H···O interactions (2.95−3.91 Å), three C−H···N interactions (3.55−3.98 Å), the multiple binding effect affords the adsorption energy of −42.07 kJ mol^{-1}. For CO_2, the terminal O atoms bind with the framework via three C = O···H (2.92−3.37 Å) and two C = O···C (3.43−3.61 Å) electrostatic interactions, while the central C atom interact with neighboring O and N atoms with distance from 3.49 to 3.89 Å, which give a sum of binding energy of −29.19 kJ mol^{-1}. Owing to the shape mismatch, C_2H_4 insert in the corner with an uncomfortable manner, and only C−H···O/N (2.93−3.54 Å) interactions can be observed, and thus gives binding energy of −24.46 kJ mol^{-1}. Taken together, the binding energy sequence of C_2H_2 > CO_2 > C_2H_4 is in good agreement with experimental findings and *in situ* IR testing (Figure S10).

The actual separation ability of **Zn-fa-mtrz** toward CO_2 and C2 mixtures was investigated by dynamic breakthrough experiments at 298 K. First, the binary CO_2/C_2H_4 (1/1, *v*/*v*) and C_2H_2/C_2H_4 (1/1, *v*/*v*) mixtures with a flow rate of 1.4 mL/min were passed through a packed column containing **Zn-fa-mtrz** (Figure 4a and 4b). C_2H_4 first elutes through the column to directly produce an outflow of pure C_2H_4 (>99.95% pure) at 59 and 61 min, respectively, while CO_2 and C_2H_2 retained in the column and detected at the outlet at 73 and 113 min, respectively. This also demonstrates the stronger affinity toward CO_2 and C_2H_2 over C_2H_4 for **Zn-fa-mtrz**, resulting in long breakthrough time intervals of 14 and 52 min, respectively. Given the excellent separation performance for binary CO_2/C_2H_4 with C_2H_2/C_2H_4 mixtures, we further test **Zn-fa-mtrz** to purify C_2H_4 from ternary $CO_2/C_2H_2/C_2H_4$ mixtures with different ratios (Figure 4c and Figure S11). As demonstrated in Figure 4c, **Zn-fa-mtrz** can effectively separate these ternary mixtures for $CO_2/C_2H_2/C_2H_4$ (1/1/1, *v*/*v*/*v*), in which C_2H_4 (99.97% pure) first elutes at 43 min, while CO_2 and C_2H_2 do not breakthrough until 53 and 71 min, respectively. When the concentration ratio of $CO_2/C_2H_2/C_2H_4$ mixtures was increased to 9:1:90 (Figure S11), **Zn-fa-mtrz** still exhibited good separation behavior, C_2H_4 (99.98% pure) flowed out at 11 min, followed by CO_2 at 21 min, and finally C_2H_2 broke through at 42 min. This result is attributed to the highly selective adsorption behavior of CO_2 and C_2H_2 over C_2H_4 in **Zn-fa-mtrz**. Moreover, the kinetic data of **Zn-fa-mtrz** for C_2H_2 and CO_2 were recorded at 298 K (Figure S12). The results showed that the diffusional rate constant of C_2H_2 (4.0698) is higher than that of CO_2 (3.5040), indicating that C_2H_2 diffused slightly faster than CO_2, indicating that in the breakthrough experiment, thermodynamic factors dominate the separation. The C_2H_4 productivity of **Zn-fa-mtrz** is calculated to be 0.484 and 1.572 mol kg^{-1} for $CO_2/C_2H_2/C_2H_4$ (1/1/1 and 9/1/90, v/v/v).

To further confirm the realistic separation property, a single adsorption bed model was built to simulate the breakthrough experiments (Figure 4). All the isotherm parameters were extracted using dual-site Langmuir−Freundlich (DSLF) model as described above and the methodology was set according to the previously established methods (see SI for detail).[48−50] The mole fraction in outlet gas was plotted in Figure 4d and 4e, for the CO_2/C_2H_4 (1/1, *v*/*v*) and C_2H_2/C_2H_4 (1/1, *v*/*v*) binary mixtures, the retention times of pure C_2H_4 were 18.8 and 42.7 min, respectively, kept in reasonable agreement with the experimental findings. For the $CO_2/C_2H_2/C_2H_4$ (1/1/1, *v*/*v*/*v*) ternary mixture, C_2H_4, CO_2, C_2H_2 were first detected at 47, 62, and 73 min (Figure 4f), the outflow order is the same with experimental breakthrough curves.

Combined with high CO_2 and C_2H_2 adsorption capacity and excellent separation performance for binary (CO_2/C_2H_4 and C_2H_2/C_2H_4) mixtures, ternary ($CO_2/C_2H_2/C_2H_4$) mixtures, **Zn-fa-mtrz** would be an exceptional material for one-step C_2H_4 purification. Subsequently, we conducted three cycles of ternary $CO_2/C_2H_2/C_2H_4$ (1/1/1) mixtures breakthrough and ten cycles of single-gas C_2H_4 adsorption experiments to assess the recyclability of **Zn-fa-mtrz** (Figure S13), with no notable performance loss after cycling.

3. CONCLUSION

In summary, we reported a pillared-layer coordination network of **Zn-fa-mtrz** with specific selective binding sites for CO_2 and C_2H_2, other than C_2H_4. The designed pore structure of **Zn-fa-mtrz** demonstrates excellent separation performance for C_2H_4, revealed by thermodynamic single-component gas adsorption and dynamic gas mixture breakthrough experiments. We believe this work will provide the useful insights to design the next-generation porous materials for complex gas mixture separation.

■ ASSOCIATED CONTENT

Supporting Information

The Supporting Information is available free of charge at https://pubs.acs.org/doi/10.1021/cbe.4c00113.

Additional experimental details; PXRD patterns; Single crystal X-ray diffraction data, TGA curve; GCMC calculations; IAST selectivity calculations; Q_{st} calculations; gas sorption measurements; and breakthrough experiments (PDF)

X-ray data for **Zn-fa-mtrz** (CIF)

■ AUTHOR INFORMATION

Corresponding Author

Kai-Jie Chen − *Xi'an Key Laboratory of Functional Organic Porous Materials, School of Chemistry and Chemical Engineering, Northwestern Polytechnical University, Xi'an, Shaanxi 710072, P. R. China;* orcid.org/0000-0001-7581-6571; Email: ckjiscon@nwpu.edu.cn

Authors

Rong Yang − *Xi'an Key Laboratory of Functional Organic Porous Materials, School of Chemistry and Chemical Engineering, Northwestern Polytechnical University, Xi'an, Shaanxi 710072, P. R. China*

Tao Zhang − *Xi'an Key Laboratory of Functional Organic Porous Materials, School of Chemistry and Chemical Engineering, Northwestern Polytechnical University, Xi'an, Shaanxi 710072, P. R. China;* orcid.org/0000-0001-9886-8411

Jinbo Wang − *Xi'an Key Laboratory of Functional Organic Porous Materials, School of Chemistry and Chemical*

https://doi.org/10.1021/cbe.4c00113
Chem Bio Eng. 2025, 2, 35−40

Engineering, Northwestern Polytechnical University, Xi'an, Shaanxi 710072, P. R. China

Xue Zhang − *Xi'an Key Laboratory of Functional Organic Porous Materials, School of Chemistry and Chemical Engineering, Northwestern Polytechnical University, Xi'an, Shaanxi 710072, P. R. China*

Jian-Wei Cao − *Xi'an Key Laboratory of Functional Organic Porous Materials, School of Chemistry and Chemical Engineering, Northwestern Polytechnical University, Xi'an, Shaanxi 710072, P. R. China;* orcid.org/0000-0003-4132-5234

Yu Wang − *Xi'an Key Laboratory of Functional Organic Porous Materials, School of Chemistry and Chemical Engineering, Northwestern Polytechnical University, Xi'an, Shaanxi 710072, P. R. China;* orcid.org/0000-0002-2296-5773

Complete contact information is available at: https://pubs.acs.org/10.1021/cbe.4c00113

Author Contributions

[+]R.Y. and T.Z. contributed equally to this work.

Notes

The authors declare no competing financial interest.

■ ACKNOWLEDGMENTS

This work was financially supported by the National Natural Science Foundation of China (No. 22071195, K.-J.C., 22101231, Y.W.), the Youth Innovation Team of Shaanxi Universities, China Postdoctoral Science Foundation (No. 2022M712585, T.Z.), and Open Project Program of State Key Laboratory of Inorganic Synthesis and Preparative Chemistry (No. 2024-28, T.Z.). We are also thankful for the help from Mr. Yuan. He, Prof. Dr. Hepeng Zhang.

■ REFERENCES

(1) Sholl, D. S.; Lively, R. P. Seven chemical separations to change the world. *Nature* **2016**, *532* (7600), 435−437.

(2) Production capacity of ethylene worldwide from 2018 to 2022. https://www.statista.com/statistics/1067372/global-ethylene-production-capacity/ (accessed 7/14/2024).

(3) Chen, K.-J.; Madden, D. G.; Mukherjee, S.; Pham, T.; Forrest, K. A.; Kumar, A.; Space, B.; Kong, J.; Zhang, Q.-Y.; Zaworotko, M. J. Synergistic sorbent separation for one-step ethylene purification from a four-component mixture. *Science* **2019**, *366* (6462), 241−246.

(4) Bao, Z.; Chang, G.; Xing, H.; Krishna, R.; Ren, Q.; Chen, B. Potential of microporous metal−organic frameworks for separation of hydrocarbon mixtures. *Energy Environ. Sci.* **2016**, *9* (12), 3612−3641.

(5) Ren, T.; Patel, M.; Blok, K. Olefins from conventional and heavy feedstocks: Energy use in steam cracking and alternative processes. *Energy* **2006**, *31* (4), 425−451.

(6) Nemati Vesali Azar, A.; Keskin, S. Computational Screening of MOFs for Acetylene Separation. *Front. Chem.* **2018**, *6*, 36.

(7) Barnett, B. R.; Gonzalez, M. I.; Long, J. R. Recent Progress Towards Light Hydrocarbon Separations Using Metal−Organic Frameworks. *Trends Chem.* **2019**, *1* (2), 159−171.

(8) Yang, S.; Ramirez-Cuesta, A. J.; Newby, R.; Garcia-Sakai, V.; Manuel, P.; Callear, S. K.; Campbell, S. I.; Tang, C. C.; Schröder, M. Supramolecular binding and separation of hydrocarbons within a functionalized porous metal−organic framework. *Nat. Chem.* **2015**, *7* (2), 121−129.

(9) Li, J.-R.; Sculley, J.; Zhou, H.-C. Metal−Organic Frameworks for Separations. *Chem. Rev.* **2012**, *112* (2), 869−932.

(10) Burtch, N. C.; Jasuja, H.; Walton, K. S. Water Stability and Adsorption in Metal−Organic Frameworks. *Chem. Rev.* **2014**, *114* (20), 10575−10612.

(11) Zhang, Z.; Tan, B.; Wang, P.; Cui, X.; Xing, H. Highly efficient separation of linear and branched C4 isomers with a tailor-made metal−organic framework. *AIChE J.* **2020**, *66* (7), No. e16236.

(12) MacGillivray, L. R.; Lukehart, C. M. *Metal-organic framework materials*; John Wiley & Sons: Chichester, U.K., 2014.

(13) Schroeder, M. *Functional metal-organic frameworks. Gas storage, separation and catalysis*; Springer: Berlin, Germany, 2010.

(14) Kitagawa, S.; Kitaura, R.; Noro, S.-i. Functional Porous Coordination Polymers. *Angew. Chem., Int. Ed.* **2004**, *43* (18), 2334−2375.

(15) Batten, S. R.; Neville, S. M.; Turner, D. R. *Coordination polymers: design, analysis and application*; Royal Society of Chemistry: 2008.

(16) Perry, J. J. t.; Perman, J. A.; Zaworotko, M. J. Design and synthesis of metal-organic frameworks using metal-organic polyhedra as supermolecular building blocks. *Chem. Soc. Rev.* **2009**, *38* (5), 1400−17.

(17) Bloch, E. D.; Queen, W. L.; Krishna, R.; Zadrozny, J. M.; Brown, C. M.; Long, J. R. Hydrocarbon separations in a metal-organic framework with open iron (II) coordination sites. *Science* **2012**, *335* (6076), 1606−1610.

(18) Liao, P.-Q.; Zhang, W.-X.; Zhang, J.-P.; Chen, X.-M. Efficient purification of ethene by an ethane-trapping metal-organic framework. *Nat. Commun.* **2015**, *6*, 8697.

(19) Li, L.; Lin, R.-B.; Krishna, R.; Li, H.; Xiang, S.; Wu, H.; Li, J.; Zhou, W.; Chen, B. Ethane/ethylene separation in a metal-organic framework with iron-peroxo sites. *Science* **2018**, *362* (6413), 443−446.

(20) Lin, R.-B.; Li, L.; Zhou, H.-L.; Wu, H.; He, C.; Li, S.; Krishna, R.; Li, J.; Zhou, W.; Chen, B. Molecular sieving of ethylene from ethane using a rigid metal−organic framework. *Nat. Mater.* **2018**, *17* (12), 1128−1133.

(21) Gu, C.; Hosono, N.; Zheng, J.-J.; Sato, Y.; Kusaka, S.; Sakaki, S.; Kitagawa, S. Design and control of gas diffusion process in a nanoporous soft crystal. *Science* **2019**, *363* (6425), 387−391.

(22) Li, Y.-P.; Zhao, Y.-N.; Li, S.-N.; Yuan, D.-Q.; Jiang, Y.-C.; Bu, X.; Hu, M.-C.; Zhai, Q.-G. Ultrahigh-Uptake Capacity-Enabled Gas Separation and Fruit Preservation by a New Single-Walled Nickel−Organic Framework. *Adv. Sci.* **2021**, *8* (12), 2003141.

(23) Geng, S.; Lin, E.; Li, X.; Liu, W.; Wang, T.; Wang, Z.; Sensharma, D.; Darwish, S.; Andaloussi, Y. H.; Pham, T.; Cheng, P.; Zaworotko, M. J.; Chen, Y.; Zhang, Z. Scalable Room-Temperature Synthesis of Highly Robust Ethane-Selective Metal−Organic Frameworks for Efficient Ethylene Purification. *J. Am. Chem. Soc.* **2021**, *143* (23), 8654−8660.

(24) Cui, X.; Chen, K.; Xing, H.; Yang, Q.-W.; Krishna, R.; Bao, Z.; Wu, H.; Zhou, W.; Dong, X.; Han, Y.; Li, B.; Ren, Q.; Zaworotko, M. J.; Chen, B. Pore chemistry and size control in hybrid porous materials for acetylene capture from ethylene. *Science* **2016**, *353* (6295), 141−144.

(25) Liao, P.-Q.; Huang, N.-Y.; Zhang, W.-X.; Zhang, J.-P.; Chen, X.-M. Controlling guest conformation for efficient purification of butadiene. *Science* **2017**, *356* (6343), 1193−1196.

(26) Zhang, Y.; Hu, J.; Krishna, R.; Wang, L.; Yang, L.; Cui, X.; Duttwyler, S.; Xing, H. Rational Design of Microporous MOFs with Anionic Boron Cluster Functionality and Cooperative Dihydrogen Binding Sites for Highly Selective Capture of Acetylene. *Angew. Chem., Int. Ed.* **2020**, *59* (40), 17664−17669.

(27) Zhang, Z.; Peh, S. B.; Wang, Y.; Kang, C.; Fan, W.; Zhao, D. Efficient Trapping of Trace Acetylene from Ethylene in an Ultramicroporous Metal−Organic Framework: Synergistic Effect of High-Density Open Metal and Electronegative Sites. *Angew. Chem., Int. Ed.* **2020**, *59* (43), 18927−18932.

(28) Dong, Q.; Huang, Y.; Hyeon-Deuk, K.; Chang, I.-Y.; Wan, J.; Chen, C.; Duan, J.; Jin, W.; Kitagawa, S. Shape- and Size-Dependent Kinetic Ethylene Sieving from a Ternary Mixture by a Trap-and-Flow Channel Crystal. *Adv. Funct. Mater.* **2022**, *32* (38), 2203745.

(29) Xue, Y.-Y.; Bai, X.-Y.; Zhang, J.; Wang, Y.; Li, S.-N.; Jiang, Y.-C.; Hu, M.-C.; Zhai, Q.-G. Precise Pore Space Partitions Combined

with High-Density Hydrogen-Bonding Acceptors within Metal−Organic Frameworks for Highly Efficient Acetylene Storage and Separation. *Angew. Chem., Int. Ed.* **2021**, *60* (18), 10122−10128.
(30) Cai, L.-Z.; Yao, Z.-Z.; Lin, S.-J.; Wang, M.-S.; Guo, G.-C. Photoinduced Electron-Transfer (PIET) Strategy for Selective Adsorption of CO2 over C2H2 in a MOF. *Angew. Chem., Int. Ed.* **2021**, *60* (33), 18223−18230.
(31) Shen, J.; He, X.; Ke, T.; Krishna, R.; van Baten, J. M.; Chen, R.; Bao, Z.; Xing, H.; Dincă, M.; Zhang, Z.; Yang, Q.; Ren, Q. Simultaneous interlayer and intralayer space control in two-dimensional metal−organic frameworks for acetylene/ethylene separation. *Nat. Commun.* **2020**, *11* (1), 6259.
(32) Fan, C. B.; Le Gong, L.; Huang, L.; Luo, F.; Krishna, R.; Yi, X. F.; Zheng, A. M.; Zhang, L.; Pu, S. Z.; Feng, X. F.; Luo, M. B.; Guo, G. C. Significant Enhancement of C2H2/C2H4 Separation by a Photochromic Diarylethene Unit: A Temperature- and Light-Responsive Separation Switch. *Angew. Chem., Int. Ed.* **2017**, *56* (27), 7900−7906.
(33) Xiang, S. C.; Zhang, Z.; Zhao, C. G.; Hong, K.; Zhao, X.; Ding, D. R.; Xie, M. H.; Wu, C. D.; Das, M. C.; Gill, R.; Thomas, K. M.; Chen, B. Rationally tuned micropores within enantiopure metal-organic frameworks for highly selective separation of acetylene and ethylene. *Nat. Commun.* **2011**, *2* (1), 1−7.
(34) Reid, C. R.; Thomas, K. M. Adsorption Kinetics and Size Exclusion Properties of Probe Molecules for the Selective Porosity in a Carbon Molecular Sieve Used for Air Separation. *J. Phys. Chem. B* **2001**, *105* (43), 10619−10629.
(35) Sircar, S. Basic Research Needs for Design of Adsorptive Gas Separation Processes. *Ind. Eng. Chem. Res.* **2006**, *45* (16), 5435−5448.
(36) Eguchi, R.; Uchida, S.; Mizuno, N. Inverse and High CO2/C2H2 Sorption Selectivity in Flexible Organic−Inorganic Ionic Crystals. *Angew. Chem., Int. Ed.* **2012**, *51* (7), 1635−1639.
(37) Dong, Q.; Zhang, X.; Liu, S.; Lin, R.-B.; Guo, Y.; Ma, Y.; Yonezu, A.; Krishna, R.; Liu, G.; Duan, J.; Matsuda, R.; Jin, W.; Chen, B. Tuning Gate-Opening of a Flexible Metal−Organic Framework for Ternary Gas Sieving Separation. *Angew. Chem., Int. Ed.* **2020**, *59* (50), 22756−22762.
(38) Mukherjee, S.; Kumar, N.; Bezrukov, A. A.; Tan, K.; Pham, T.; Forrest, K. A.; Oyekan, K. A.; Qazvini, O. T.; Madden, D. G.; Space, B.; Zaworotko, M. J. Amino-Functionalised Hybrid Ultramicroporous Materials that Enable Single-Step Ethylene Purification from a Ternary Mixture. *Angew.Chem. Int. Ed.* **2021**, *60* (19), 10902−10909.
(39) Li, X.; Ding, Q.; Liu, J.; Dong, L.; Qin, X.; Zhou, L.; Zhao, Z.; Ji, H.; Zhang, S.; Chai, K. One-step ethylene purification from ternary mixtures by an ultramicroporous material with synergistic binding centers. *Mater. Horiz.* **2023**, *10* (10), 4463−4469.
(40) Jiang, Y.; Hu, Y.; Luan, B.; Wang, L.; Krishna, R.; Ni, H.; Hu, X.; Zhang, Y. Benchmark single-step ethylene purification from ternary mixtures by a customized fluorinated anion-embedded MOF. *Nat. Commun.* **2023**, *14* (1), 401.
(41) Jiang, X.; Pham, T.; Cao, J.-W.; Forrest, K. A.; Wang, H.; Chen, J.; Zhang, Q.-Y.; Chen, K.-J. Molecular Sieving of Acetylene from Ethylene in a Rigid Ultra-microporous Metal Organic Framework. *Chem.—Eur. J.* **2021**, *27* (36), 9446−9453.
(42) Wang, L.; Zhang, Y.; Zhang, P.; Liu, X.; Xiong, H.; Krishna, R.; Liu, J.; Shuai, H.; Wang, P.; Zhou, Z.; Chen, J.; Chen, S.; Deng, S.; Wang, J. Electro-field alignment in a novel metal−organic framework for benchmark separation of ethylene from a ternary gas mixture. *AIChE J.* **2024**, *70*, e18396.
(43) Cao, J. W.; Mukherjee, S.; Pham, T.; Wang, Y.; Wang, T.; Zhang, T.; Jiang, X.; Tang, H. J.; Forrest, K. A.; Space, B.; Zaworotko, M. J.; Chen, K. J. One-step ethylene production from a four-component gas mixture by a single physisorbent. *Nat. Commun.* **2021**, *12* (12), 6507.
(44) Yang, R.; Wang, Y.; Cao, J.-W.; Ye, Z.-M.; Pham, T.; Forrest, K. A.; Krishna, R.; Chen, H.; Li, L.; Ling, B.-K.; Zhang, T.; Gao, T.; Jiang, X.; Xu, X.-O.; Ye, Q.-H.; Chen, K.-J. Hydrogen bond unlocking-driven pore structure control for shifting multi-component gas separation function. *Nat. Commun.* **2024**, *15* (1), 804.
(45) Spek, A. L. Single-crystal structure validation with the program PLATON. *J. Appl. Crystallogr.* **2003**, *36* (1), 7−13.
(46) Wang, J.; Lian, X.; Zhang, Z.; Liu, X.; Zhao, Q.; Xu, J.; Cao, X.; Li, B.; Bu, X.-H. Thiazole functionalized covalent triazine frameworks for C_2H_6/C_2H_4 separation with remarkable ethane uptake. *Chem. Commun.* **2023**, *59* (75), 11240−11243.
(47) Wang, J.; Lian, X.; Cao, X.; Zhao, Q.; Li, B.; Bu, X.-H. Dual polarization strategy to enhance CH_4 uptake in covalent organic frameworks for coal-bed methane purification. *Chin. Chem. Lett.* **2024**, *35* (8), 109180.
(48) Krishna, R. Screening metal−organic frameworks for mixture separations in fixed-bed adsorbers using a combined selectivity/capacity metric. *RSC Adv.* **2017**, *7* (57), 35724−35737.
(49) Krishna, R. Methodologies for screening and selection of crystalline microporous materials in mixture separations. *Sep. Purif. Technol.* **2018**, *194*, 281−300.
(50) Krishna, R. Metrics for Evaluation and Screening of Metal−Organic Frameworks for Applications in Mixture Separations. *ACS Omega* **2020**, *5* (28), 16987−17004.

https://doi.org/10.1021/cbe.4c00113
Chem Bio Eng. 2025, 2, 35−40